

OPTIMIZATION OF THERMOFORMING WITH PROCESS MODELLING

*R. DiRaddo, D. Laroche and A. Bendada
Industrial Materials Institute
National Research Council of Canada
Boucherville, Quebec, Canada*

and

*T. Ots
Quality Thermoform
Etobicoke, Ontario, Canada*

Abstract

The thermoforming process involves three stages, sheet rehear, forming and solidification. A polymeric sheet is heated in an oven to the desired forming temperature distribution. The sheet is then deformed to take the shape of the mould cavity and subsequently solidified.

This work includes the modelling and experimental validation of both the sheet rehear and vacuum forming stages. The part considered is moulded in a box shape cavity mould that is supplied by Quality Thermoform. The modelling simulations and the corresponding experimental trials were performed at the Industrial Materials Institute. The heat transfer in the oven is modelled by employing combined radiation and natural convection. The sheet forming is modelled with a non-isothermal viscoelastic constitutive equation. The process stages are modelled in sequence, namely sheet rehear, sag and vacuum forming.

Introduction

Thermoforming of cut sheets is extensively used in the industry for various commercial applications. The market for the thermoforming process is significantly expanding to more complex geometries and new materials, since the process results in lower residual stress levels and lower tooling costs than injection moulding. Product development times must be reduced to accommodate new global market requirements. Furthermore, the product development phase must include an initial step for material selection and mould geometry determination, based on costs, properties and processability criteria (1).

Process modelling technologies are useful tools in achieving the desired product development goals. Process modelling technologies assist the product development by predicting the dependence of final part

quality on operating conditions, tooling and part design as well as material properties. The use of process modelling technologies is also important for the reduction of process set-up times and tooling costs. However, prior to the employment of process modelling technologies in the product development stage, confidence must be built regarding the quality of the predictions.

The objective of this work is to model and experimentally validate the sheet rehear and forming stages of the thermoforming process. The thermoformed part quality depends on the heating stage, and therefore an integrated modelling approach that consecutively predicts sheet rehear and forming is proposed. The simulation takes into account the oven operating conditions, including heater-sheet geometry and source temperature distributions, to calculate the sheet temperature evolution as well as the sheet sag. The results are used to simulate the sheet deformation that occurs in the forming stage. The simulation predictions are compared to experimental results obtained on an industrial scale thermoforming machine. Measurements of the sheet temperature at the exit of the oven, as well as the final part thickness distribution are individually validated.

The use of sensitivity analysis for the optimization of the process is also demonstrated. The sheet temperature in individual zones is perturbed in a controlled fashion so as to determine the effects on the final part thickness distribution. The sensitivity analysis is performed both experimentally and numerically.

Theory

Proper simulation of the entire thermoforming process combines heat transfer and viscoelastic deformations. The sheet is meshed using triangular finite elements with a multi-layer membrane formulation. The triangular element also includes a heat

transfer calculation across the thickness of the sheet. The heat transfer analysis couples radiation and convection boundary conditions on both sides of the sheet. The predicted temperature distribution is applied to every layer of the sheet and affects the stress/strain behaviour of the material. A non-isothermal viscoelastic formulation is used to represent the sheet deformation due to a gravity load or an applied pressure. Therefore the thermal and sag predictions are coupled in the reheat stage.

The same fundamentals as the sheet reheat and sag calculations are employed during forming. The boundary conditions and loading are simply replaced. Air convection of the forming station replaces the radiation heating while vacuum, pressure and plug travel are added to the gravity load.

The first stage of the thermoforming process involves the heating of the sheet to a softened state. Simulation of this stage requires accurate modelling of the heat flux received by the polymer sheet. The total heat flux q_{tot} at the sheet surface is a combination of radiation and convection and is given by:

$$q_{tot} = q_{rad} + h(T_{air} - T) \quad (1)$$

where q_{rad} is the radiative heat flux incident on the surface and h is the air convection coefficient. The heat flux q_{rad} depends on the oven configuration including the relative position of the heaters, the heater source temperature profiles, the effective emissivity of the heater-polymer system as well as sheet position in the oven. The incident radiant heat is either absorbed, reflected or transmitted depending on the material under consideration. For an opaque material such as ABS, the transmittance is negligible and the absorbance is generally between 90 and 100 %. The absorbed energy is subsequently conducted through the thickness of the sheet.

To calculate the radiative heat flux incident on the sheet surface, the oven is modelled with triangular elements representing the zone surfaces. The global radiative heat flux received by the sheet becomes the summation of each heater element contribution according to the following equation:

$$q_{rad} = \sum_i \sigma \epsilon_{eff,i} A_i F_i (T_i^4 - T^4) \quad (2)$$

where σ is the Stefan-Boltzmann constant, A is the individual source element surface area, F is the corresponding view factor and T is the source element temperature. The radiative efficiency of the sheet-polymer system is ϵ_{eff} . Radiative exchanges with other oven components are neglected. Correct modelling of the air convection is also important since it affects the sheet surface temperature.

The efficiency, ϵ_{eff} , is the product of the effective emissivity of the sheet-heater system and the fraction of the absorbed energy. For ABS and ceramic heaters the effective emissivity is approximately 0.85 (2) and therefore the efficiency ϵ_{eff} ranges from 0.70 to 0.85.

The sheet sag as well as the sheet forming are predicted with the K-BKZ viscoelastic constitutive model combined with the WLF shift function to account for temperature dependence. The K-BKZ model is derived from the BKZ family and is generally accepted as the best performing model for representing polymer deformations in the molten state. The BKZ model relates the stress to the strain history by the use of an energy function U as follows (3,4).

$$\sigma(t) = -qId + 2 \int_{-\infty}^t \left(F(t, \tau) \frac{\partial U}{\partial C(t, \tau)} F^T(t, \tau) / J(t, \tau) \right) d\tau \quad (3)$$

With the use of an energy equation, the BKZ constitutive equation can be transformed to the K-BKZ model (5,6).

$$\sigma = -qId + \frac{1}{1-\theta} \int_{-\infty}^t m(t-\tau) h(I_1, I_2) (c^{-1}(\tau, t) + \theta c(\tau, t)) d\tau \quad (4)$$

where m is a memory function given by the Maxwell relaxation spectrum, h is a damping function based on the Cauchy strain invariants and θ refers to the second normal stress difference in the deformation (biaxial effect).

The thermal dependence of the K-BKZ model is accounted for with a temperature shift function that modifies the modulus or the relaxation times of viscoelastic models. The most common shift function used is the WLF equation.

$$\ln(a_T) = -\frac{c_1(T - T_{ref})}{c_2 + T - T_{ref}} \quad (5)$$

where c_1 and c_2 are model constants and T_{ref} is the reference temperature at which the shift a_T equals 1.

An important advantage of thermoforming modelling technologies is the ability to perform a sensitivity analysis. Such an analysis gives the relationships between the operating conditions and the part quality. The procedure consists of the manipulation of every input parameter in order to establish an overall sensitivity matrix. The number of parameters becomes very important and therefore numerical simulation is useful for non-linear and multi-variable systems.

In this work, an example of sensitivity analysis for the optimization of the process is demonstrated. The heater temperature in individual zones is perturbed in a controlled fashion so as to determine the effects on the

final part thickness distribution. This results in the determination of a Jacobian matrix J that relates the variation of the heater temperature profile to the part thickness distribution as follow:

$$\delta h_i = J_i \delta T, \quad (6)$$

where δh_i is the part thickness variation and δT_i is the temperature variation of the heater zones. The Jacobian matrix can be determined either experimentally or numerically. The inversion of matrix J can then be used to determine corrections to the heater temperature profile that yield a new part thickness distribution. The influence of every parameter is usually non-linear and consequently, the Jacobian matrix is valid only for small size corrections. When large modifications of the operating conditions are required, the Jacobian matrix is ideally recalculated. When the off-diagonal components of the matrix are large relative to the diagonal components, the system is said to be coupled. Both non-linear and coupled situations complicate optimization.

Experimental

The experiments were performed on an AAA industrial scale thermoforming machine. The material considered is ABS Lustran 752. The sheet dimensions are 25.4 cm width, 38.1 cm length and 0.159 cm thickness. The sheet is clamped on all four sides. The material is dried for 60 minutes prior to processing. The operating conditions employed in the study are shown in Table 1.

The oven has an upper bank of six ceramic elements for profiled control of three zones. Each element has dimensions 30.5 cm width by 9.5 cm length. The distance from the sheet to the heaters is kept constant at 6.0 cm. The air temperature in the oven was measured with a thermocouple and was found to be approximately 60 °C.

The sheet surface temperature distribution at the end of the heating stage, was measured with an AGEMA 900LW infra-red camera. The sheet was kept in the oven for a sufficient time (180 seconds) to ensure a steady state temperature across the thickness of the sheet. A typical sheet temperature distribution for a constant heater setting profile is shown in Figure 1. As expected, the temperature of the sheet is higher in the centre of the sheet than in the extremities. This is a result of the view factor distribution in the sheet-heater configuration. Also discontinuities are present at the separation points of the individual heaters. The sheet temperature distribution is non-uniform, even for a constant heater profile setting, resulting in forming with a complex sheet deformation response and consequently an unpredictable thickness distribution.

The mould geometry considered for the forming analysis is a 31.3 cm by 16.9 cm box with a depth of 9.62 cm. Figure 2 shows the cross-sectional cut of the mould where the thickness distribution were measured. Validation experiments were performed on ABS samples thermoformed using the operating conditions given in Table 1.

Results and Discussion

Integrated simulations of sheet reheat, sag and forming were performed. The sheet mesh has a total of 13,440 elements and 6893 nodes. The number of nodes in the sheet is elevated, to ensure an adequate prediction of the part thickness in the corners of the box, where the highest blow ratios occurred. A profiled heater setting is considered to validate the ability of the numerical simulation to represent the effect of complex oven settings. Stagnant air is assumed for natural convection. Table 2 summarizes the material thermal properties and oven parameters employed in the reheat simulation. Three reheat simulations using radiative efficiencies of 0.70, 0.80 and 0.95 were performed to verify its effect on the sheet temperature evolution.

Figure 3 compares the predicted temperature profiles to the experimental temperature profile obtained for the cross-section being studied. As expected, the average temperature level in the sheet increases with increasing heater efficiencies. A heater efficiency of 0.70 gives the best comparison to the experimental results. Also there is a discrepancy between the predicted and experimental temperature results at the extremities of the sheet. This can be attributed to end effects caused by the clamping frame behaving like a heat sink.

Table 3 summarizes the K-BKZ non-isothermal viscoelastic properties for ABS. The material data is obtained with a RMS mechanical spectrometer. The predicted sheet deflection due to sag was 3.2 cm. These results compared well to the experimental measurements which range from 3 to 4 cm. Simulation of the forming stage was performed using the predicted sheet temperature distribution of Figure 3. The mesh of the mould cavity surface has a total of 6338 elements and 3203 nodes. Figure 4 shows the predicted sheet deformation steps of the forming simulation where the degree of shading represents the thickness distribution.

Figure 5 shows the experimental validation of the simulation prediction for the forming analysis. These results show good agreement of the predicted part thickness with the measurements. The prediction in the centre of the part is adequate. The simulation underpredicts the thickness at the extremities. This can be attributed to cooling of the sheet by conduction heat transfer near the clamping bars. This cooling results in higher sheet rigidity at the extremities and therefore a thicker thickness is experimentally obtained. This is

believed to be the principal cause of the discrepancy in the thickness results.

A sensitivity analysis was performed to study the effect of oven set-up on the part wall thickness distribution. The output parameters under consideration are the average thickness of the part in three zones. The input parameters are the ceramic element temperatures of the three zones. Figures 6 and 7 show the effect of heater profiling on the final part thickness distribution, for simulation predictions and experimental results, respectively. Increasing the left heater temperature results in thinner wall thickness in this area. The assumption that hotter regions deform and consequently thin out more is confirmed both numerically and experimentally. However, the coupling effects between the three zones are difficult to interpret. This can be attributed to the high level of non-linearity in the system. The discrepancy between the predicted and measured temperature distribution, observed in Figure 3, can affect the numerical simulation's ability to represent the effect of profiled heating. High dependency on the temperature of the viscoelastic properties and potential sheet slip along cavity walls can also contribute to the system non-linearity. Both the experimental and numerical analyses confirmed that the degree of coupling is elevated.

Conclusion

In this work, the numerical and experimental techniques for the optimization of the thermoforming process were investigated. A numerical model predicting the sheet temperature distribution after reheat, combining radiation and convection heat transfer, is proposed. The experimental measurements show that the model is capable of representing the effect of oven settings. Finite element simulations of sheet sag and forming were also presented. The predicted part thickness distribution agreed well with the experimental measurements on thermoformed samples made of ABS. A sensitivity analysis using the proposed integrated process simulation was demonstrated. The results agreed well with experimental results.

Acknowledgement

The authors would like to acknowledge the technical contributions of Dominic Brunelle, Christian duGrandpré, Anna Bardetti and Linda Pecora in this work. The contributions of the members of the SIGFORM group is also recognized.

References

1. M.F. Howery, *SPE ANTEC Tech Paper*, 43, p.698 (1997).
2. J.L. Thorne, *Plastics Engineering*, 37 (1998).
3. C. Truesdell, *J. Ratl. Mech. Anal.*, 2, p.125 (1952).

4. B. Bernstein et al., *Trans. Soc. Rheol.*, 7, p.391 (1963).
5. B.A. Kaye, *Non-Newtonian Flow Incompressible Fluids*, College of Aeronautics, Cranfield, p.134 (1962).
6. R.I. Turner, *Engineering Rheology*, Clarendon Press, Oxford (1985).

Table 1: Operating conditions.

Operating conditions	
Sheet heating time	180 sec
Sheet transfer time	2.0 sec
Evacuation time	5.0 sec
Mould cooling time	10.0 sec
Mould cooling temperature	30 °C
Forming pressure	Full vacuum

Table 2: Material thermal properties and oven parameters.

Density	1050.0 Kg/m ³
Conductivity	0.18 W/m/°C
Specific heat	1300 J/Kg/°C
Air temperature in the oven	60.0 °C
Natural convection coefficient	10.0 W/m ² /°C
Heater setting profile	335-270-270 °C

Table 3: Non-isothermal viscoelastic properties

Relaxation modulus (MPa)	Relaxation time (sec)
0.063316	0.00893
0.101389	0.0625
0.055233	0.437
0.023620	3.06
0.005340	21.4
0.005943	150.0
WLF constants	
T _g (°C)	170.
c ₁	16.43
c ₂ (°C)	300.

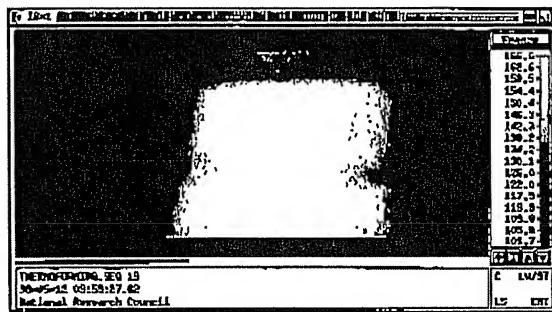


Figure 1: Measured sheet temperature distribution.

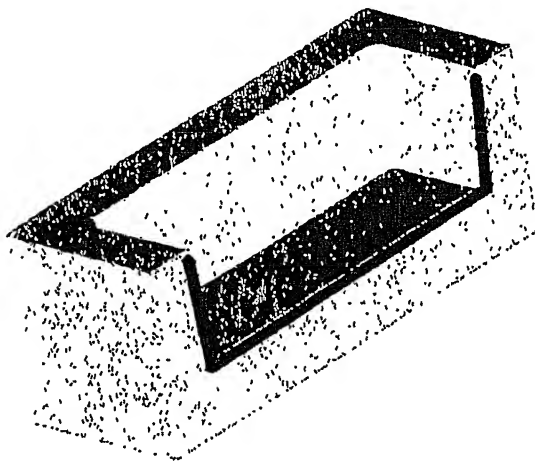


Figure 2: Cut section of the mould cavity.

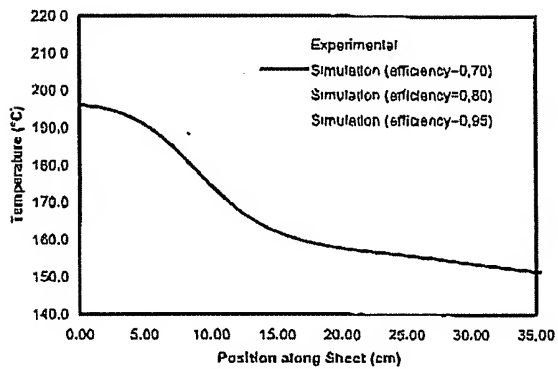


Figure 3: Experimental validation of the reheat simulation.

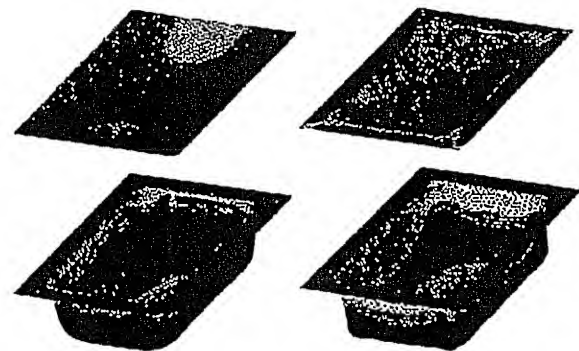


Figure 4: Steps in the forming analysis

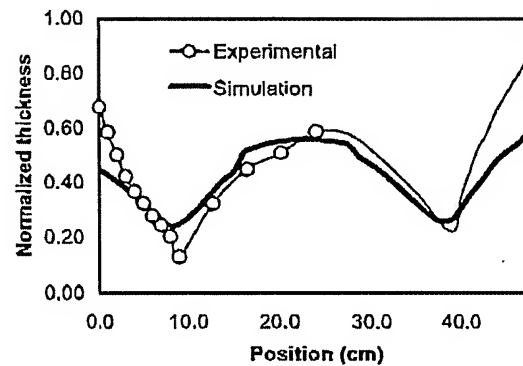


Figure 5: Experimental validation of the forming simulation.

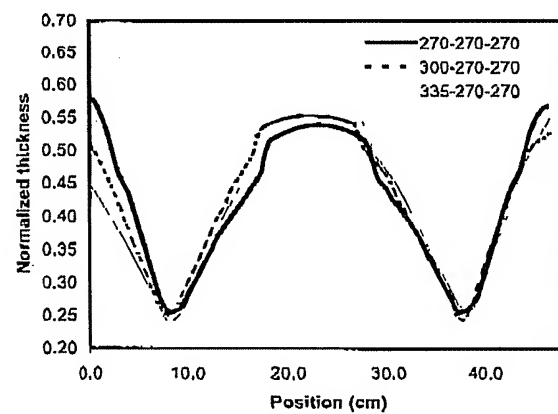


Figure 6: Predicted effect of heater profiling.

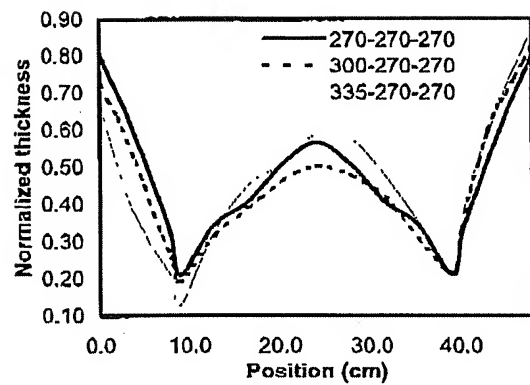


Figure 7: Experimental effect of heater profiling.